

THE JOURNAL OF PHARMACOLOGY AND EXPERIMENTAL THERAPEUTICS

American Society for Pharmacology and Experimental Therapeutics

[J Pharmacol Exp Ther](#). 2010 Feb; 332(2): 569–577.

PMCID: PMC2819831

doi: [10.1124/jpet.109.159145](https://doi.org/10.1124/jpet.109.159145)

PMID: [19906779](https://pubmed.ncbi.nlm.nih.gov/19906779/)

Cannabidiol Displays Antiepileptiform and Antiseizure Properties In Vitro and In Vivo^{S□}

[Nicholas A. Jones](#), [Andrew J. Hill](#), [Imogen Smith](#), [Sarah A. Bevan](#), [Claire M. Williams](#), [Benjamin J. Whalley](#), and [Gary J. Stephens](#)[✉]

School of Pharmacy (N.A.J., A.J.H., I.S., S.A.B., B.J.W., G.J.S.) and School of Psychology (N.A.J., A.J.H., C.M.W.), University of Reading, Whiteknights, Reading, United Kingdom

[✉]Corresponding author.

Address correspondence to: Dr. Gary Stephens, School of Pharmacy, University of Reading, Whiteknights, P.O. Box 228, Reading RG6 6AJ, UK., E-mail: g.j.stephens@reading.ac.uk

Received 2009 Jul 22; Accepted 2009 Nov 9.

[Copyright](#) © 2010 by The American Society for Pharmacology and Experimental Therapeutics

Abstract

Plant-derived cannabinoids (phytocannabinoids) are compounds with emerging therapeutic potential. Early studies suggested that cannabidiol (CBD) has anticonvulsant properties in animal models and reduced seizure frequency in limited human trials. Here, we examine the antiepileptiform and antiseizure potential of CBD using in vitro electrophysiology and an in vivo animal seizure model, respectively. CBD (0.01–100 μ M) effects were assessed in vitro using the Mg^{2+} -free and 4-aminopyridine (4-AP) models of epileptiform activity in hippocampal brain slices via multielectrode array recordings. In the Mg^{2+} -free model, CBD decreased epileptiform local field potential (LFP) burst amplitude [in CA1 and dentate gyrus (DG) regions] and burst duration (in all regions) and increased burst frequency (in all regions). In the 4-AP model, CBD decreased LFP burst amplitude (in CA1 only at 100 μ M CBD), burst duration (in CA3 and DG), and burst frequency (in all regions). CBD (1, 10, and 100 mg/kg) effects were also examined in vivo using the pentylenetetrazole model of generalized seizures. CBD (100 mg/kg) exerted clear anticonvulsant effects with significant decreases in incidence of severe seizures and mortality compared with vehicle-treated animals. Finally, CBD acted with only low affinity at cannabinoid CB_1 receptors and displayed no agonist activity in [35 S]guanosine 5'-O-(3-thio)triphosphate assays in cortical membranes. These findings suggest that CBD acts, potentially in a CB_1 receptor-independent manner, to inhibit epileptiform activity in vitro and seizure severity in vivo. Thus, we demonstrate the potential of CBD as a novel antiepileptic drug in the unmet clinical need associated with generalized seizures.

A growing number of phytocannabinoids have been shown to possess biological activity ([Pertwee, 2008](#)) and, in particular, to affect neuronal excitability in the CNS. Phytocannabinoid actions are reported to be mediated by G protein-coupled cannabinoid CB_1 and CB_2 receptors and potentially by other non-CB receptor targets ([Howlett et al., 2004](#); [Pertwee, 2008](#)). CB_1 receptors are highly expressed in the hippocampus ([Herkenham et al., 1990](#); [Tsou et al., 1998](#)) and are well known to

modulate epileptiform and seizure activity ([Shen and Thayer, 1999](#); [Wallace et al., 2001](#)). Moreover, the endocannabinoid (eCB) system has been shown to be a key determinant of hippocampal epileptiform activity ([Wallace et al., 2002](#); [Monory et al., 2006](#); [Ludányi et al., 2008](#)). The major psychoactive compound Δ^9 -THC was the first phytocannabinoid reported to affect epileptiform activity; Δ^9 -THC, a partial agonist at CB₁ receptors, was shown to inhibit excitatory glutamatergic neurotransmission in hippocampal neurons under low Mg²⁺ conditions ([Shen and Thayer, 1999](#); but see [Straiker and Mackie, 2005](#)).

CBD is the major nonpsychoactive component of *Cannabis sativa* whose structure was first described by [Mechoulam and Shvo \(1963\)](#); CBD has recently attracted renewed interest for its therapeutic potential in a number of disease states ([Pertwee, 2008](#)). CBD has been proposed to possess anticonvulsive, neuroprotective, and anti-inflammatory properties in humans. Thus, within the CNS, CBD has been proposed to be protective against epilepsy, anxiety, and psychosis and to ameliorate diseases of the basal ganglia, such as parkinsonism and Huntington's disease ([Iuvone et al., 2009](#); [Scuderi et al., 2009](#)). CBD neuroprotective effects may be augmented by reported antioxidant properties ([Hampson et al., 1998](#); [Sagredo et al., 2007](#)). Early studies suggested that CBD had anticonvulsant potential in one small-scale phase I clinical trial ([Cunha et al., 1980](#)). In this regard, there is a significant unmet clinical need for epilepsy, with ~30% of epileptic patients experiencing intractable seizures regardless of conventional AED treatment ([Kwan and Brodie, 2007](#)). CBD is extremely well tolerated in humans; for example, CBD at doses of 600 mg does not precipitate any of the psychotic symptoms associated with Δ^9 -THC ([Bhattacharyya et al., 2009](#)). At present, CBD is used therapeutically in Sativex (1:1 Δ^9 -THC/CBD; GW Pharmaceuticals, Porton Down, UK) to alleviate pain symptoms in multiple sclerosis and cancer pain. CBD has anticonvulsant effects in animal models of maximal electroshock ([Karler et al., 1974](#); [Consroe and Wolkin, 1977](#); [Consroe et al., 1982](#)); however, CBD remains untested in other animal seizure models ([Gordon and Devinsky, 2001](#)) and so has yet to fulfill its potential indications as a clinical anticonvulsant.

In the present study, we demonstrate the potential of CBD as an AED. We show that CBD caused concentration-related and region-dependent attenuation of chemically induced epileptiform activity in hippocampal brain slices using in vitro MEA electrophysiological recordings. Furthermore, CBD reduced seizure severity and mortality in an in vivo model of generalized seizures. We also investigated the specific role of CB₁ receptors in CBD action and found only a low-affinity interaction and lack of clear agonist effects. Overall, these data are consistent with CBD acting to mediate antiepileptiform and antiseizure effects in vitro and in vivo, respectively, potentially by CB₁ receptor-independent mechanisms.

Materials and Methods

In Vitro Electrophysiology

Tissue Preparation and Solutions. All experiments were performed in accordance with Home Office regulations [Animals (Scientific Procedures) Act 1986]. Acute transverse hippocampal brain slices (~450 μ m thick) were prepared from male and female (postnatal day \geq 21) Wistar Kyoto rats using a Vibroslice 725M (Campden Instruments Ltd., Loughborough, Leicestershire, UK). Slices were produced and maintained in continuously carboxygenated (95% O₂-5% CO₂) artificial cerebrospinal fluid (aCSF) composed of 124 mM NaCl, 3 mM KCl, 1.25 mM KH₂PO₄, 1 mM MgSO₄ · 6H₂O, 36 mM NaHCO₃, 2 mM CaCl₂, and 10 mM *d*-glucose, pH 7.4. Spontaneous epileptiform activity was induced either by exchange of the standard aCSF perfusion media for aCSF with MgSO₄ · 6H₂O removed (Mg²⁺-free aCSF) or by addition of the K⁺ channel blocker 4-AP (100 μ M; 4-AP aCSF).

MEA Electrophysiological Recording.

Substrate-integrated MEAs (Multi Channel Systems, Reutlingen, Germany) ([Egert et al., 2002a](#); [Stett et al., 2003](#)) were used to record spontaneous neuronal activity as described previously ([Ma et al., 2008](#)). MEAs were composed of 60 electrodes (including reference ground) of 30 μm diameter, arranged in an $\sim 8 \times 8$ array with 200 μm spacing between electrodes.

MEAs were cleaned before each recording by immersion in 5% w/v Terg-A-Zyme (Cole-Palmer, London, UK) in distilled H_2O , followed by methanol, and, finally, distilled H_2O before air drying. Hippocampal sections immersed in aCSF were gently microdissected away from surrounding slice tissue using fine forceps under a WILD M8 binocular microscope (Leica AG, Solms, Germany). Dissected hippocampi were then adhered to the cleaned MEA surface using an applied and evaporated cellulose nitrate solution in methanol ($\sim 4 \mu\text{l}$, 0.24% w/v; Thermo Fisher Scientific, Leicestershire, UK) to ensure maximum contact between the tissue and recording electrodes and to avoid any physical stress on the tissue during recordings. Slices were observed at $4\times$ magnification with a Nikon TS-51 inverted microscope (Nikon, Tokyo, Japan) and imaged via a Mikro-Okular camera (Bresser, Rhede, Germany) to map electrode positions to hippocampal regions. Slices were maintained at 25°C , continuously superfused ($\sim 2 \text{ ml/min}$) with carboxygenated aCSF, and allowed to stabilize for at least 10 min before recordings. Signals were amplified ($1200\times$ gain), band pass-filtered (2–3200 Hz) by a 60-channel amplifier (MEA60 System, Multi Channel Systems), and simultaneously sampled at 10 kHz per channel on all 60 channels. Data were transferred to PC using MC_Rack software (Multi Channel Systems). Offline analysis of CBD effects upon burst amplitude, duration, and frequency was performed using MC_Rack, MATLAB 7.0.4. (Mathworks Inc., Natick, MA) and in-house analysis scripts. Animated contour plots of MEA-wide neuronal activity (Supplemental Fig. 1) were constructed from raw data files processed in MATLAB 6.5 using in-house code with functions adapted from MEA Tools and interpolated using a five-point Savitzky-Golay filter in MATLAB ([Egert et al., 2002b](#)). These data are displayed as peak source and peak sink animation frames. Burst propagation speeds were calculated by determining burst peak times at electrode positions closest to burst initiation (CA3) and termination (CA1) sites using MC_Rack and ImageJ software ([Abramoff et al., 2004](#)).

Data Presentation and Statistics. Application of Mg^{2+} -free and 4-AP aCSF induced spontaneous epileptiform activity characterized by recurrent status epilepticus-like local field potential (LFP) events ([Figs. 2, A and B, and 4, A and B](#)). We have recently characterized and validated the use of MEA technology to screen candidate AEDs in the Mg^{2+} -free and 4-AP models using reference compounds, felbamate and phenobarbital ([Hill et al., 2009](#)). A discrete burst was defined as an LFP with both positive and negative components of greater than 2 S.D. from baseline noise. In each model, LFPs were abolished by the addition of the non-NMDA glutamate receptor antagonist 6-nitro-7-sulfamoylbenzo(*f*)quinoxaline-2–3-dione (5 μM) and tetrodotoxin (TTX, 1 μM) ($n = 3$ per model), indicating that epileptiform activity was due to firing of hippocampal neurons. After an initial 30-min control period, CBD was added cumulatively in increasing concentrations (30 min each concentration). Burst parameters (amplitude, duration, and frequency) were determined from the final 10 bursts of the control period or of each drug concentration. Increases in burst amplitude and decreases in frequency inherent to both in vitro models were observed over time in recordings in the absence of CBD ($n = 4$ per model). These changes required appropriate compensation to allow accurate assessment of CBD effects and have been rigorously modeled by us recently ([Hill et al., 2009](#)). Thus, burst frequency and amplitude from control recordings were normalized to the values observed after 30 min of epileptiform activity, then pooled to give mean values. Curves were fitted to resultant data, and derived equations were used to adjust values obtained from recordings in the presence of CBD. For amplitude; $y = 0.8493 \times e^{(x \times -0.009295)} + 0.4216$ for Mg^{2+} -free-induced bursting ($r^2 = 0.98$) and $y = 0.87 \times e^{(-x/83.32)} + 0.45$ for 4-AP-induced bursting ($r^2 = 0.99$), where $x = \text{time}$ and $y = \text{burst amplitude}$. Frequency changes were more complex and required fifth-order polynomial equations: $y = -9e^{-14x^4} + 7e^{-10x^3} - 3e^{-06x^2} + 0.006x - 3.594$ for Mg^{2+} -free-induced bursting ($r^2 = 0.818$); and $y = 5^{-14x^4} - 5e^{-10x^3} + 2e^{-06x^2} -$

$0.004x + 3.965$ for 4-AP-induced bursting ($r^2 = 0.915$), where $x = \text{time}$ and $y = \text{frequency}$ (Hill et al., 2009). Inevitable dead cell debris on the slice surface produced slice-to-slice variability in signal strength. Consequently, drug-induced changes are presented as changes to the stated measure versus control per experiment to provide normalized measures for pooled data. Statistical significance was determined by a nonparametric two-tailed Mann-Whitney U test. Mean propagation speeds (meters per second) were derived from pooled data and the significance of drug effects was tested using a two-tailed Student's t test. In all cases, $P \leq 0.05$ was considered significant.

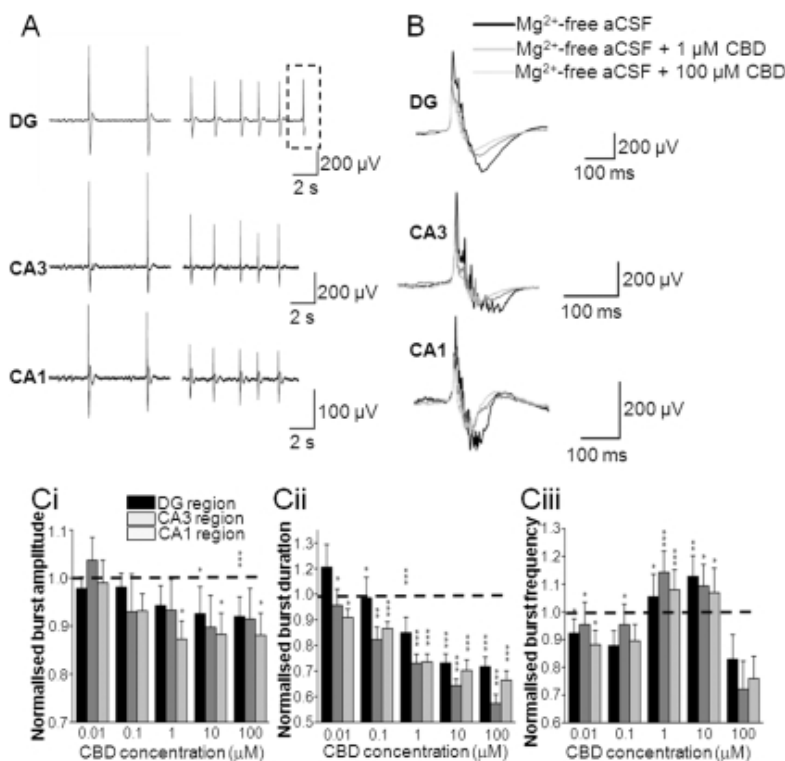


Fig. 2.

CBD attenuates epileptiform activity induced by Mg^{2+} -free aCSF. A, representative traces showing the effects of 100 μM CBD on Mg^{2+} -free aCSF-induced LFP bursts in different regions of hippocampal slices. Dotted lines represent an individual LFP (as shown in B). B, effects of 1 and 100 μM CBD on a representative individual Mg^{2+} -free aCSF-induced LFP burst. C, bar graphs showing the effects of acute treatment of increasing CBD concentrations on normalized burst amplitude (Ci), normalized burst duration (Cii), and normalized burst frequency in Mg^{2+} -free aCSF (Ciii). Note that burst amplitudes have been adjusted for run-down and burst frequencies have been adjusted for run-up as described under *Materials and Methods*. Values are means \pm S.E.M. for the last 10 LFP bursts in each condition. *, $P \leq 0.05$; **, $P \leq 0.01$; ***, $P \leq 0.001$ (two-tailed Mann-Whitney U test).

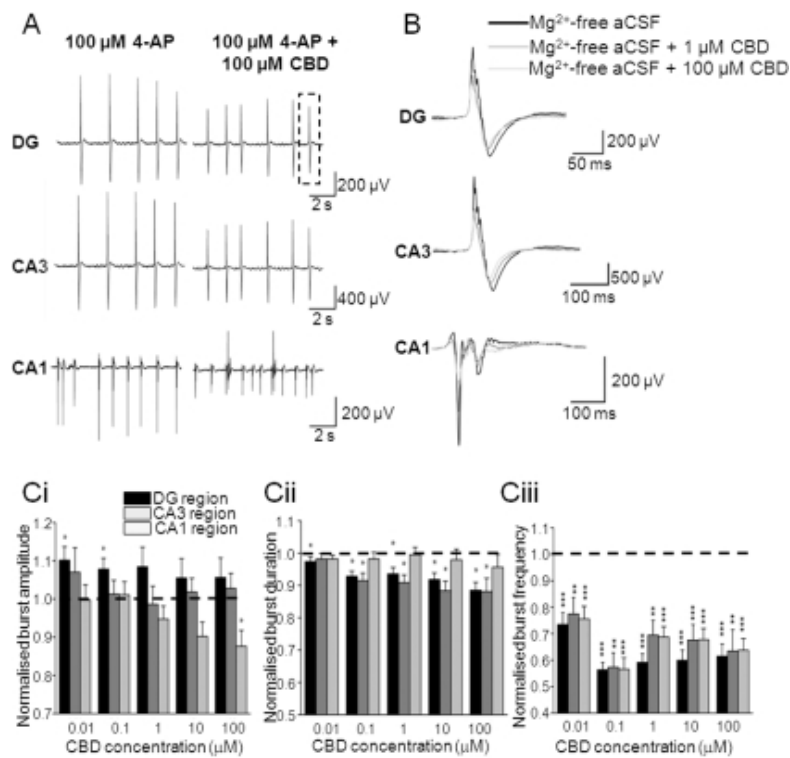


Fig. 4.

CBD attenuates epileptiform activity induced by 4-AP aCSF. A, representative traces showing effects of 100 μM CBD on 4-AP aCSF-induced LFP bursts in different regions of a hippocampal slice. Dotted lines represent an individual LFP (as shown in B). B, effects of 1 and 100 μM CBD on a representative individual 4-AP aCSF-induced LFP burst. C, bar graphs showing the effects of acute treatment of increasing CBD concentrations on normalized burst amplitude (Ci), normalized burst duration (Cii), and normalized burst frequency in the 4-AP aCSF (Ciii). Note that burst amplitudes have been adjusted for run-down and burst frequencies have been adjusted for run-up as described under *Materials and Methods*. Values are means \pm S.E.M. for the last 10 LFP bursts in each condition. *, $P \leq 0.05$; **, $P \leq 0.01$; ***, $P \leq 0.001$ (two-tailed Mann-Whitney U test).

Pharmacology. The following agents were used: 6-nitro-7-sulfamoylbenzo(*f*)quinoxaline-2-3-dione (Tocris Cookson, Bristol, UK), tetrodotoxin (Alomone, Jerusalem, Israel), and 4-AP (Sigma-Aldrich, Poole, UK). CBD was kindly provided by GW Pharmaceuticals. CBD was made up as a 1000-fold stock solution in dimethylsulfoxide (Thermo Fisher Scientific, Leicestershire, UK) and stored at -20°C . Individual aliquots were thawed and dissolved in carboxygenated aCSF immediately before use. In all experiments, drugs were bath-applied (2 ml/min) for 30 min to achieve steady-state effects after the induction of epileptiform activity.

Pentylentetrazole in Vivo Seizure Model

PTZ (80 mg/kg; Sigma-Aldrich) was used to induce seizures in 60 adult (postnatal day >21 , 70–110 g) male Wistar Kyoto rats. In the days before seizure induction, animals were habituated to handling, experimental procedures, and the test environment. Before placement in their observation arenas, animals were injected intraperitoneally with CBD (1, 10, or 100 mg/kg); vehicle was a 1:1:18 solution of ethanol, Cremophor (Sigma-Aldrich), and 0.9% w/v NaCl. CBD is known to penetrate the blood-

brain barrier such that 120 mg/kg delivered intraperitoneally in rats provides $C_{\max} = 6.8 \mu\text{g/g}$ at $T_{\max} = 120$ min and, at the same dosage, no major toxicity, genotoxicity, or mutagenicity was observed (personal communication via GW Pharmaceuticals Ltd; Study Report UNA-REP-02). A group of animals that received volume-matched doses of vehicle alone served as a negative control. Sixty minutes after CBD or vehicle administration, animals were injected with 80 mg/kg PTZ i.p. to induce seizures. An observation system using closed-circuit television cameras ([Farrimond et al., 2009](#)) was used to monitor the behavior of up to five animals simultaneously from CBD/vehicle administration until 30 min after seizure induction. Input from closed-circuit TV cameras was managed and recorded by Zoneminder (version 1.2.3; Triornis Ltd., Bristol, UK) software and then was processed to yield complete videos for each animal.

Seizure Analysis. Videos of PTZ-induced seizures were scored offline with a standard seizure severity scale appropriate for generalized seizures ([Pohl and Mares, 1987](#)) using Observer Video-Pro software (Noldus, Wageningen, The Netherlands). The seizure scoring scale was divided into stages as follows: 0, no change in behavior; 0.5, abnormal behavior (sniffing, excessive washing, and orientation); 1, isolated myoclonic jerks; 2, atypical clonic seizure; 3, fully developed bilateral forelimb clonus; 3.5, forelimb clonus with tonic component and body twist; 4, tonic-clonic seizure with suppressed tonic phase with loss of righting reflex; and 5, fully developed tonic-clonic seizure with loss of righting reflex ([Pohl and Mares, 1987](#)).

Specific markers of seizure behavior and development were assessed and compared between vehicle control and CBD groups. For each animal the latency (in seconds) from PTZ administration to the first sign of a seizure, development of a clonic seizure, development of tonic-clonic seizures, and severity of the seizure were recorded. In addition, the median severity, percentage of animals that experienced the highest seizure score (stage 5: tonic-clonic seizure), and percent mortality for each group were determined. Mean latency \pm S.E.M. are presented for each group, together with the median value for seizure severity. Differences in latency and seizure duration values were assessed using one-way analysis of variance with a post hoc Tukey test; Mann-Whitney U tests were performed when replicant (n) numbers were insufficient to support post hoc testing. Differences in seizure incidence and mortality (percentage) were assessed by a nonparametric binomial test. In all cases, $P \leq 0.05$ was considered to be significant.

Receptor Binding Assays

Membrane Preparation. Cortical tissue was dissected from the brains of adult (postnatal day >21) male and female Wistar Kyoto rats and stored separately at -80°C until use. Tissue was suspended in a membrane buffer, containing 50 mM Tris-HCl, 5 mM MgCl_2 , 2 mM EDTA, and 0.5 mg/ml fatty acid-free bovine serum albumin (BSA) and complete protease inhibitor (Roche, Mannheim, Germany), pH 7.4, and was then homogenized using an Ultra-Turrax blender (Labo Moderne, Paris, France). Homogenates were centrifuged at 1000g at 4°C for 10 min, and supernatants were decanted and retained. Resulting pellets were rehomogenized and centrifugation was repeated as before. Supernatants were combined and then centrifuged at 39,00g at 4°C for 30 min in a high-speed Sorvall centrifuge; remaining pellets were resuspended in membrane buffer, and protein content was determined by the method of [Lowry et al. \(1951\)](#). All procedures were carried out on ice.

Radioligand Binding Assays. Competition binding assays against the CB_1 receptor antagonist [^3H]SR141716A rimonabant were performed in triplicate in assay buffer containing 20 mM HEPES, 1 mM EDTA, 1 mM EGTA, and 5 mg/ml fatty acid-free BSA, pH 7.4. All stock solutions of drugs and membrane preparations were diluted in assay buffer and stored on ice immediately before incubation. Assay tubes contained 0.5 nM [^3H]SR141716A ($K_d = 0.53 \pm 0.01$ nM, $n = 3$, determined from saturation assay curves) together with drugs at the desired final concentration and were made up to a

final volume of 1 ml with assay buffer. Nonspecific binding was determined in the presence of the CB₁ receptor antagonist AM251 (10 μM). Assays were initiated by addition of 50 μg of membrane protein. Assay tubes were incubated for 90 min at 25°C, and the assay was terminated by rapid filtration through Whatman GF/C filters using a Brandell cell harvester, followed by three washes with ice-cold phosphate-buffered saline to remove unbound radioactivity. Filters were incubated overnight in 2 ml of scintillation fluid, and radioactivity was quantified by liquid scintillation spectrometry.

[³⁵S]GTPγS Binding Assays. Assays were performed in triplicate in assay buffer containing 20 mM HEPES, 3 mM MgCl₂, 60 mM NaCl, 1 mM EGTA, and 0.5 mg/ml fatty acid-free BSA, pH 7.4. All stock solutions of drugs and membrane preparations were diluted in assay buffer and stored on ice immediately before use. Assay tubes contained GDP at a final concentration of 10 mM, together with drugs at the desired final concentration and were made up to a final volume of 1 ml with assay buffer. Assays were initiated by addition of 10 μg of membrane protein. Assays were incubated for 30 min at 30°C before addition of [³⁵S]GTPγS (final concentration 0.1 nM). Assays were terminated after a further 30-min incubation at 30°C by rapid filtration through Whatman GF/C filters using a Brandell cell harvester, followed by three washes with ice-cold phosphate-buffered saline to remove unbound radioactivity. Filters were incubated for a minimum of 2 h in 2 ml of scintillation fluid, and radioactivity was quantified by liquid scintillation spectrometry.

Data Analysis and Statistical Procedures. Data analyses were performed using GraphPad Prism (version 4.03; GraphPad Software Inc., San Diego, CA). Saturation experiments were performed to determine K_d and B_{max} (picomoles per milligram) values; the free radioligand concentration was determined by subtraction of total bound radioligand from the added radioligand concentration. Data for specific radioligand binding and free radioligand concentration were fitted to equations describing one- or two-binding site models, and the best fit was determined using an F test. Saturation analyses best fit a one-binding site model. Competition experiments were fitted to one- and two-binding site models, and the best fit was determined using an F test. Data for the best fits are expressed as K_i values, with the respective percentage of high-affinity sites (percent R_H) given for two-binding site models (Vivo et al., 2006). The Hill slope for competition experiments was determined using a sigmoidal concentration-response model (variable slope). [³⁵S]GTPγS concentration-response data were analyzed using a sigmoidal concentration-response model (variable slope) or linear regression and compared using an F test to select the appropriate model. No other constraints were applied. [³⁵S]GTPγS binding is expressed as percentage increase in radioactivity as described previously (Dennis et al., 2008). All data are expressed as mean ± S.E.M.

Pharmacology. The following agents were used: AM251, WIN55,212-2 (Tocris-Cookson, Bristol, UK), CBD (GW Pharmaceuticals), and [³H]SR141716A and [³⁵S]GTPγS (GE Healthcare, Chalfont St. Giles, Buckinghamshire, UK). All other reagents were from Sigma-Aldrich.

Results

Characterization of Mg²⁺-Free and 4-AP Models of Epileptiform Activity Using MEA Electrophysiology. To investigate neuronal excitability in vitro, we used both the Mg²⁺-free and 4-AP models of epileptiform activity in acute hippocampal brain slices, as measured using MEA electrophysiology. Two separate models of epileptiform activity were used to provide a broader analysis of drug effects (Hill et al., 2009; Whalley et al., 2009). Hippocampal slices have a well defined architecture (Fig. 1A), exhibited no spontaneous LFP events in control aCSF, and proved readily amenable to MEA recording (Fig. 1B). We sought to take advantage of the ability of MEAs to record spatiotemporal activity at multiple discrete, identifiable regions by investigating activity at CA1, CA3, and DG regions within the hippocampus. Application of Mg²⁺-free aCSF (Fig. 1C) or 4-AP aCSF (Fig. 1D) to hippocampal slices resulted in the appearance of robust spontaneous epileptiform LFPs across the preparation. LFPs were

consistent with status epilepticus-like activity and were reliably recorded using the multisite MEA technique (Table 1). Slice-to-slice variability and electrode contact variability resulted in substantial variation in signal strength (Table 1); therefore, subsequent drug-induced changes in burst characteristics were normalized to control bursts before drug application (these analyses are fully characterized in Hill et al., 2009).

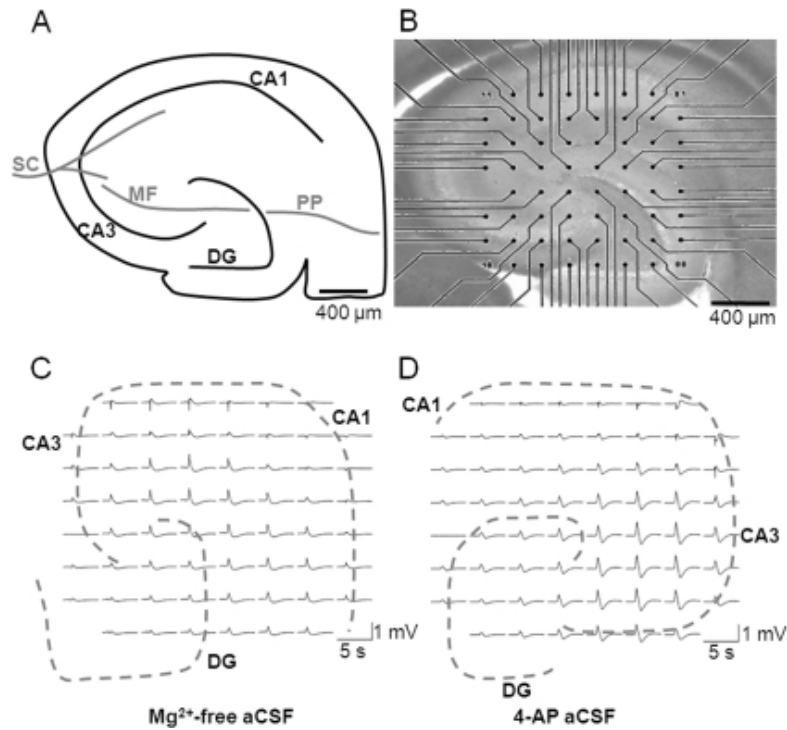


Fig. 1.

Hippocampal slices are amenable to MEA recording. A, schematic representation of hippocampal slice showing the position of CA1, CA3, and DG regions, together with major pathways: Schaffer collateral (SC), mossy fiber (MF), and perforant pathway (PP). B, micrograph showing a hippocampal brain slice (stained with pontamine blue) mounted onto a substrate-integrated MEA (60 electrodes of 30 μm diameter, spaced 200 μm apart in an ~8 × 8 arrangement). Scale bar, 400 μm. Representative LFP burst activity was recorded at 60 electrodes across a hippocampal slice in (C) Mg²⁺-free aCSF and (D) 4-AP aCSF. Traces were high pass-filtered in an MC_rack at 2 Hz.

Table 1

Characterization measures for the Mg^{2+} -free and 4-AP (100 μM) aCSF-induced LFP epileptiform activity in the CA1, CA3, and DG regions of the hippocampus

LFP peak burst amplitude values are presented as a minimum and maximum range and mean \pm S.E.M. LFP burst duration and frequencies are presented as mean \pm S.E.M. A minimum of six separate hippocampal slices were used in the characterisation of each in vitro model.

In Vitro Model	Hippocampal Region	LFP Peak Burst Amplitude			LFP Burst Duration	LFP Burst Frequency
		Minimum	Maximum	Mean \pm S.E.M.		
			μV		<i>ms</i>	<i>Hz</i>
Mg^{2+} -free	CA1 ($n = 15$)	77	438	257 ± 30	747 ± 29	0.31 ± 0.01
	CA3 ($n = 12$)	37	971	303 ± 88	722 ± 31	0.30 ± 0.02
	DG ($n = 15$)	66	781	275 ± 53	715 ± 28	0.30 ± 0.02
4-AP (100 μM)	CA1 ($n = 15$)	54	383	201 ± 26	508 ± 21	0.77 ± 0.08
	CA3 ($n = 13$)	13	1218	364 ± 101	524 ± 19	0.71 ± 0.07
	DG ($n = 18$)	44	674	338 ± 44	552 ± 12	0.75 ± 0.06

Effects of CBD in the Mg^{2+} -Free Model of in Vitro Epileptiform Activity. We first examined the effects of CBD in the Mg^{2+} -free model to assess CBD effects on a receptor-dependent model of epileptiform activity. The Mg^{2+} -free model removes the Mg^{2+} -dependent block of NMDA glutamate receptors, rendering them more responsive to synaptically released glutamate at resting membrane potentials. In Mg^{2+} -free aCSF, CBD significantly decreased LFP burst amplitude in the CA1 (1–100 μM CBD) and DG (10–100 μM CBD) regions (Fig. 2, A, B, and Ci). In contrast, CBD (0.01–100 μM) effects on LFP burst amplitude in CA3 failed to reach significance. CBD decreased burst duration in CA1 (0.01–100 μM CBD), CA3 (0.01–100 μM CBD), and DG (0.1–100 μM CBD) regions (Fig. 2, A, B, and Cii). CBD (0.01–10 μM) also caused an increase in burst frequency in all regions tested (Fig. 2Ciii; however, this effect was lost at 100 μM CBD). To correlate these data with information on LFP burst initiation and spread across the hippocampal brain slice, we constructed contour plots (Fig. 3A) and associated video animations (Supplemental Fig. 1). Such plots spatiotemporally visualize the “ 8×8 ” MEA configuration (Fig. 1, B and C) and the individual LFP activity shown in raw data traces (Fig. 2, A and B). In these experiments, Mg^{2+} -free aCSF-induced bursts typically originated in the CA3 region of the hippocampal slice preparation and propagated along the principal cell layer toward CA1. LFP events induced by Mg^{2+} -free aCSF had a mean propagation speed of 0.229 ± 0.048 m/s ($n = 6$). CBD (100 μM) caused a clear suppression of Mg^{2+} -free-induced LFP burst amplitude peak source and peak sink values across the hippocampal slice (Fig. 3A; Supplemental Fig. 1). Propagation speed across the brain slice in Mg^{2+} -free aCSF was not affected by 100 μM CBD (0.232 ± 0.076 m/s; $n = 6$; $P > 0.5$).

Taken together, these data suggest that, although CBD attenuates epileptiform LFP amplitude and duration in the Mg^{2+} -free model, the rate of signal spread across the preparation is not changed (see *Discussion*).

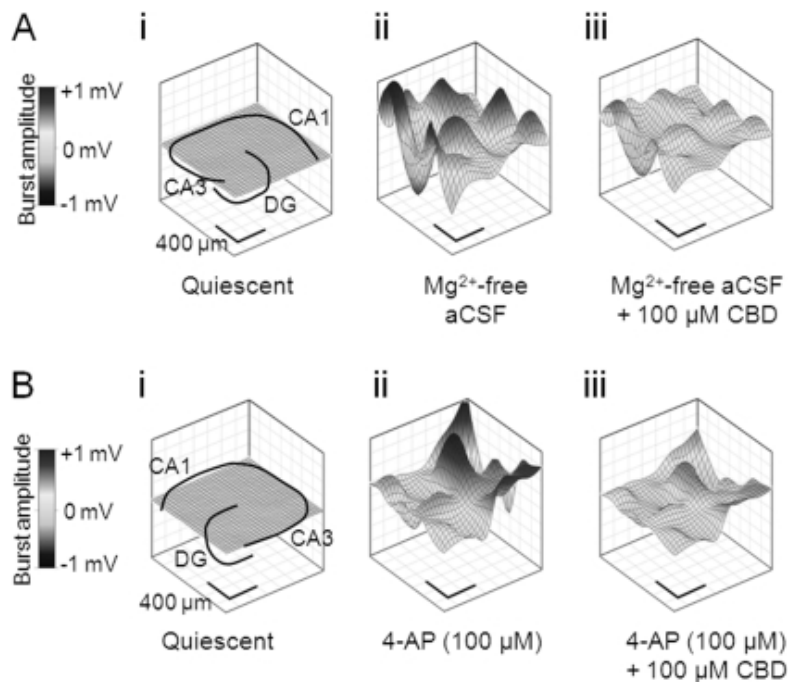


[Fig. 3.](#)

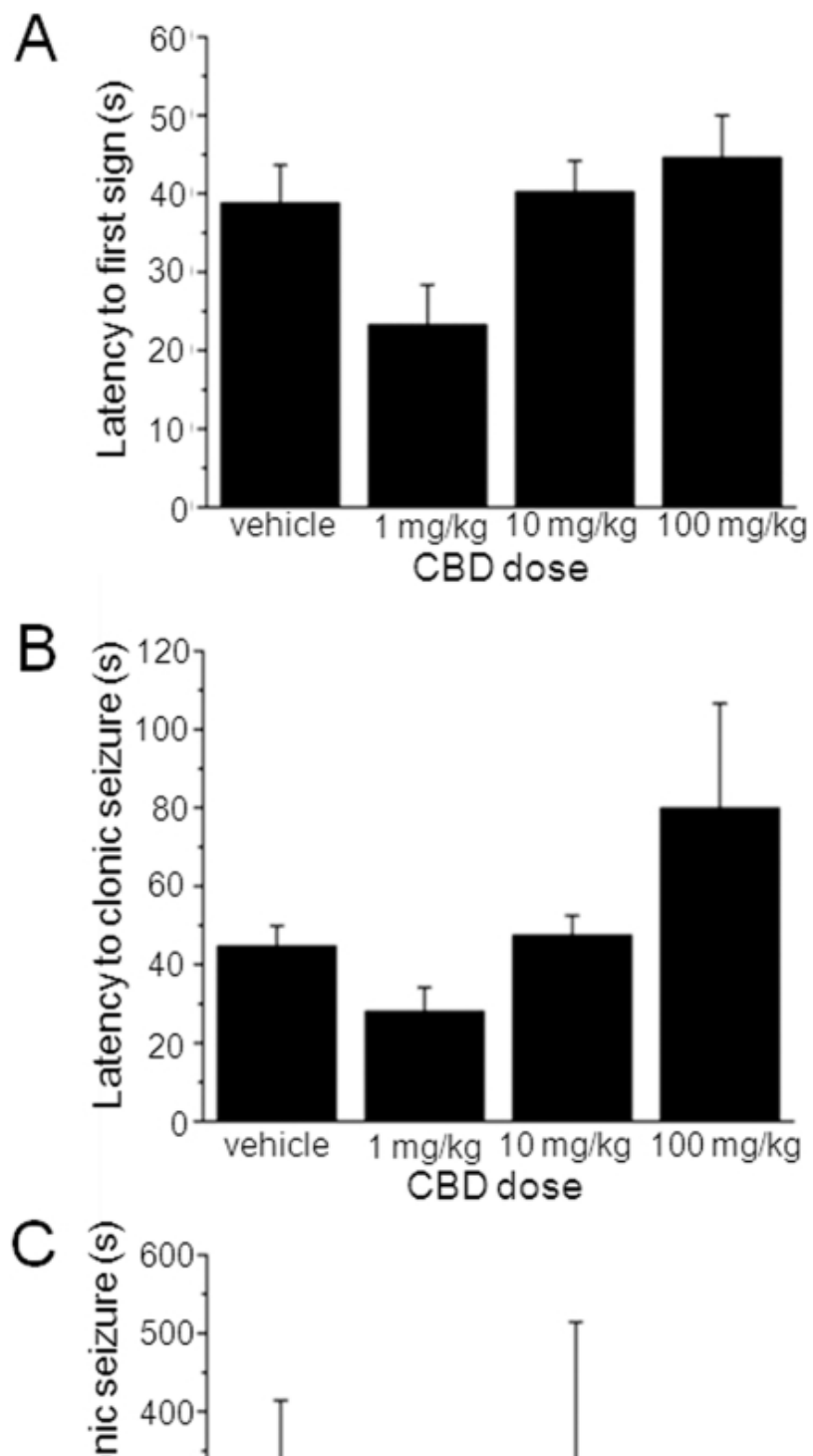
CBD attenuates epileptiform activity induced by Mg^{2+} -free and 4-AP aCSF. Representative contour plots illustrating CBD effects upon spatiotemporal epileptiform burst features. A, in the continued presence of Mg^{2+} -free aCSF: quiescent period between epileptiform burst events also showing hippocampal slice orientation (i), peak source in the absence of CBD (ii), and peak source in the presence of CBD (100 μ M) (iii). B, in the continued presence of 100 μ M 4-AP: quiescent period between epileptiform burst events also showing hippocampal slice orientation (i), peak source in the absence of CBD (ii), and peak source in the presence of CBD (100 μ M) (iii).

Effects of CBD in the 4-AP Model of in Vitro Epileptiform Activity. We next examined the effects of CBD on epileptiform bursting events in the 4-AP model of status epilepticus-like activity. 4-AP acts to block postsynaptic voltage-dependent K^+ channels and inhibits neuronal repolarization to effectively increase excitability. In 100 μ M 4-AP aCSF, CBD (100 μ M) caused a significant decrease in LFP burst amplitude in CA1 only ([Fig. 4](#), A, B, and Ci). In contrast, CBD (0.01–0.1 μ M) caused an unexpected small, but significant, increase in LFP burst amplitude in the DG, which was not apparent at higher CBD concentrations in this or other hippocampal regions ([Fig. 4Ci](#)). CBD caused a decrease in burst duration in the DG (0.01–100 μ M CBD) and CA3 (0.1–100 μ M CBD) but was without an overall effect on CA1 ([Fig. 4](#), A, B, and Cii). CBD (0.01–100 μ M) also caused a significant decrease in burst frequency in all regions tested ([Fig. 4Ciii](#)). In the same manner as for the Mg^{2+} -free model, contour plots of 4-AP-induced epileptiform LFP burst events ([Fig. 3B](#)) permitted spatiotemporal visualization of activity across the slice preparation (Supplemental Fig. 1). 4-AP aCSF-induced bursts typically were initiated in CA3 before spreading to CA1 with a propagation speed of 0.146 ± 0.033 m/s ($n = 5$). CBD

(100 μ M) caused a clear suppression of 4-AP-induced epileptiform LFP burst amplitude ([Fig. 3B](#); Supplemental Fig. 1). Propagation speed across the brain slice in 4-AP aCSF was not affected by 100 μ M CBD (0.176 ± 0.046 m/s, $n = 6$; $P > 0.5$).

Taken together, these data show that CBD displayed clear concentration-related, region-specific, anticonvulsant properties in two different in vitro models of epileptiform activity, attenuating LFP burst amplitude and duration, but with no effect on the rate of signal propagation in either model.

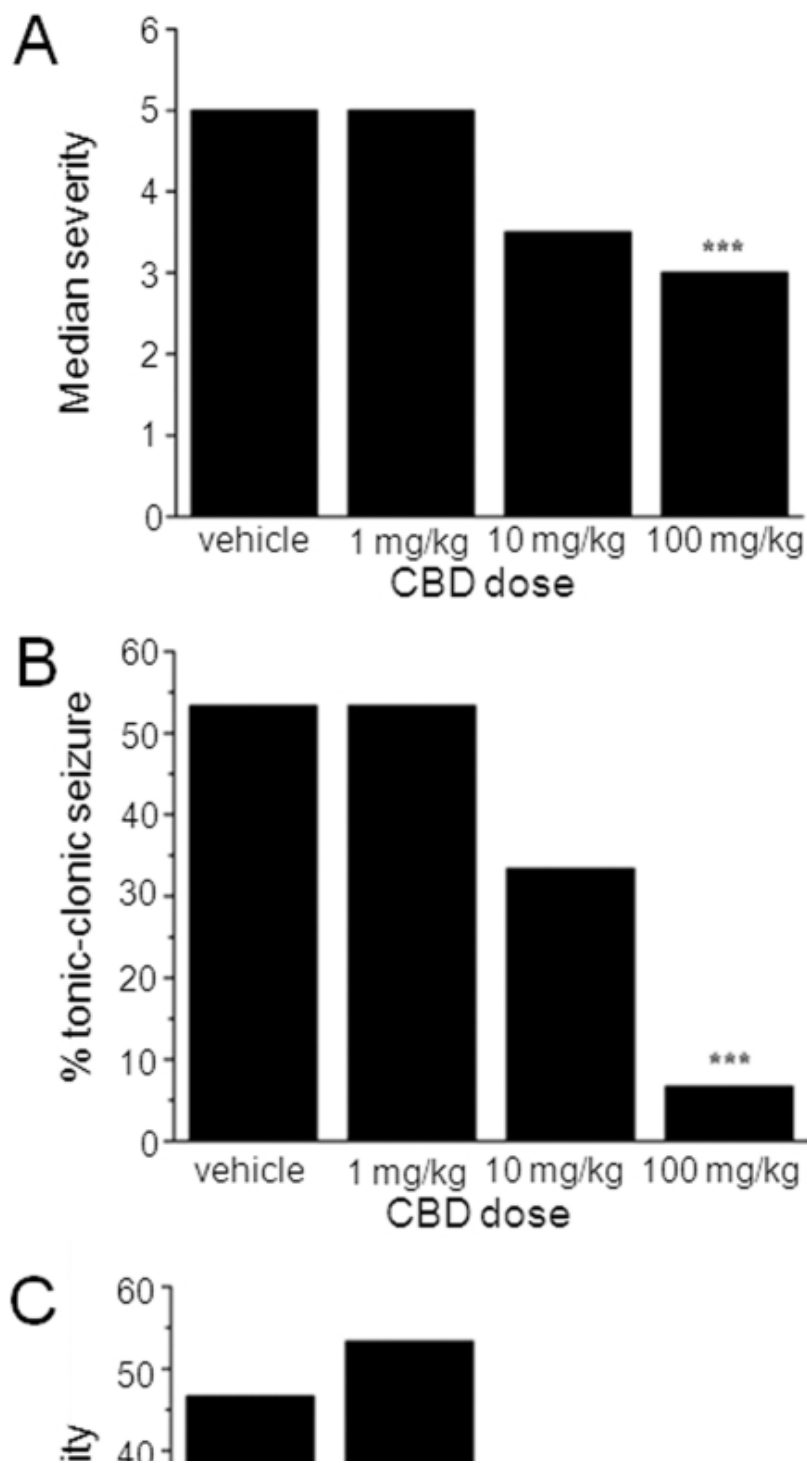
Effects of CBD in the PTZ Model of Generalized Seizures. We next assessed the effects of CBD (1, 10, and 100 mg/kg i.p.) on PTZ-induced generalized seizures in adult male rats. PTZ acts as a GABA_A receptor antagonist and this model is well defined and used as a standard for the identification of potential anticonvulsants to treat generalized clonic seizures ([Löscher et al., 1991](#)). Seizures were defined by a standard scoring scale (see *Materials and Methods*). CBD at any dose did not significantly alter the latency to the first sign of PTZ-induced seizures ([Fig. 5A](#)) or latency to development of clonic ([Fig. 5B](#)) seizures. Unexpectedly, CBD (1 mg/kg) reduced latency to tonic-clonic seizures ($P < 0.01$) ([Fig. 5C](#)). No other effects of CBD on latency to specific seizure states were observed. In contrast to the lack of definitive effects on seizure latency, CBD (100 mg/kg) demonstrated clear anticonvulsant effects via measures of seizure severity ([Fig. 6, A and B](#)) and mortality ([Fig. 6C](#)). When the severity of PTZ-induced seizures is considered, vehicle-treated animals reached a median score of 5 (tonic-clonic seizures with a loss of righting reflex), the most severe on the scoring scale ([Fig. 6A](#)). In contrast, animals treated with 100 mg/kg CBD exhibited a significantly reduced median score of 3.5 (forelimb clonus with a tonic component, but with the righting reflex preserved; $n = 15$ animals; $P < 0.001$) ([Fig. 6A](#)). This was associated with a marked decrease in the proportion of animals that developed the most severe tonic-clonic seizures, which was reduced from 53% in vehicle to 7% by 100 mg/kg CBD ($n = 15$ animals, $P < 0.001$) ([Fig. 6B](#)). Finally, percent mortality was significantly reduced from 47% in vehicle to 7% by 100 mg/kg CBD ($n = 15$ animals, $P < 0.001$) ([Fig. 6C](#)). Overall, these in vivo data confirm our in vitro results above and fully support an anticonvulsant action for CBD.



[Open in a separate window](#)

Fig. 5.

CBD has no clear effects on seizure latency in vivo. Bar graphs showing lack of effects of CBD (1, 10, and 100 mg/kg) on latency to the first sign of a seizure (A), latency to clonic seizures (B), and latency to tonic-clonic seizures (C). Each data set $n = 15$ animals. Note that CBD (1 mg/kg) reduced latency to tonic-clonic seizures; this proconvulsant action was not observed at higher CBD doses. **, $P \leq 0.01$ (one-way analysis of variance) with a post hoc Tukey test).



[Open in a separate window](#)

Fig. 6.

CBD reduces seizure severity and mortality in vivo. Bar graphs showing effects of CBD (1, 10, and 100 mg/kg) on median seizure severity (A), percentage of animals reaching tonic-clonic seizures (B), and percent mortality (C). Each data set $n = 15$ animals. CBD (100 mg/kg) significantly reduced all of these parameters: ***, $P \leq 0.001$ (nonparametric binomial test).

It is known that hippocampal CB₁ receptor expression on glutamatergic terminals is selectively down-regulated under epileptic conditions ([Ludányi et al., 2008](#)); moreover, activation of CB₁ receptors by eCBs is protective against seizures ([Monory et al., 2006](#)) and exogenous CB₁ agonists decrease epileptiform activity in hippocampal neurons ([Shen and Thayer, 1999](#); [Blair et al., 2006](#)). Therefore, we determined potential CBD actions at CB₁ receptors. Competition binding assays were performed for CBD against the CB₁ receptor antagonist [³H]SR141716A in isolated cortical membranes; CBD effects were compared with those of the standard synthetic CB receptor agonist WIN55,212-2 and the CB₁ receptor antagonist AM251 ([Fig. 7A](#)). AM251 displacement of [³H]SR141716A binding occurred with high affinity ($K_i = 190 \pm 56$ pM; $n = 4$) and was best fitted by a one-site competition model (Hill slope = -1.08 ± 0.13 ; $n = 4$). In contrast, WIN55,212-2 displacement was best fitted to a two-site model with a high-affinity site ($K_i = 7.03 \pm 4.1$ nM; % $R_h = 27.4 \pm 5.0\%$; $n = 4$) and a low-affinity site ($K_i = 904 \pm 155$ nM; $n = 4$); in these experiments, Hill slopes for either the low- or high-affinity site did not match unity. CBD displacement of [³H]SR141716A occurred with low affinity ($K_i = 1.82 \pm 0.38$ μ M; $n = 4$) and was best fitted by a one-site model (Hill slope = -1.15 ± 0.11 ; $n = 4$).

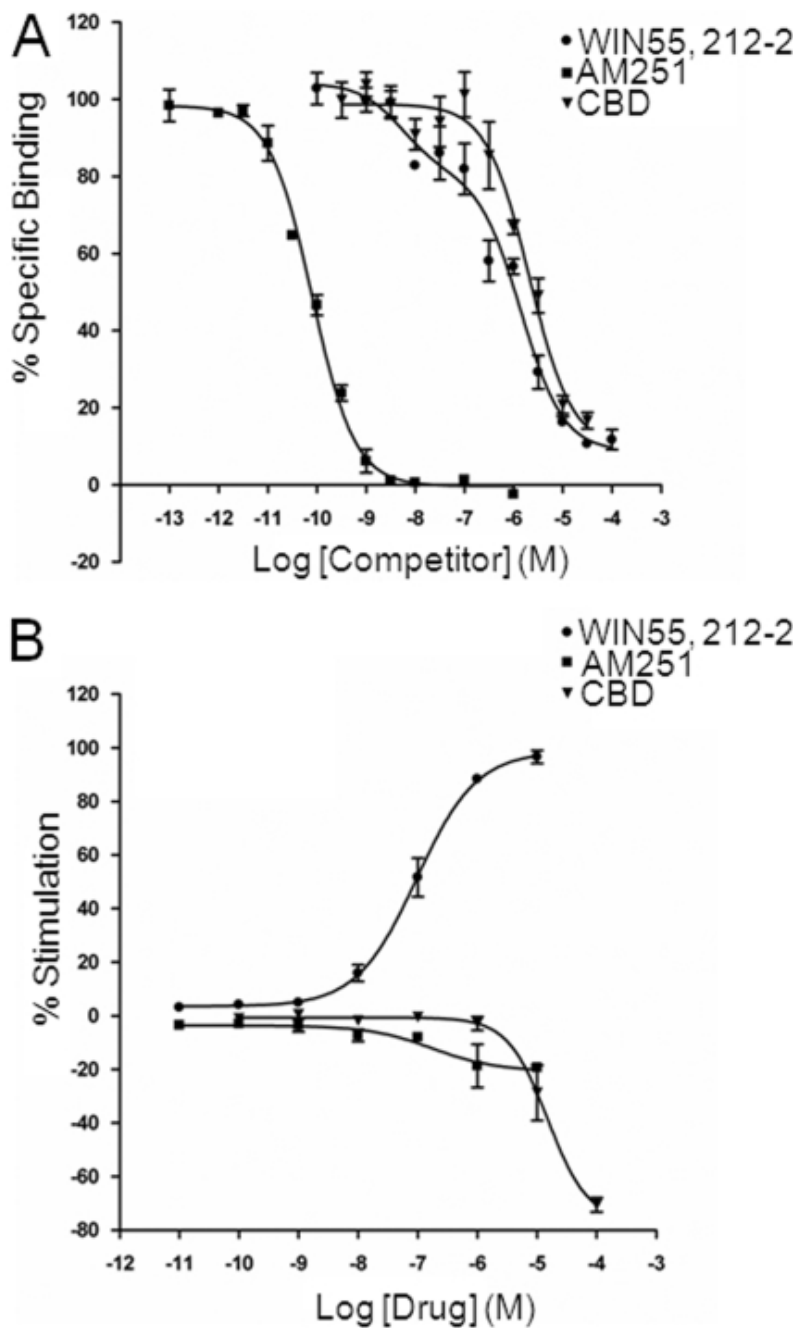


[Fig. 7.](#)

CBD displaces [^3H]SR141716A binding with low affinity and lacks agonist effects in [^{35}S]GTP γ S binding assays in cortical membranes. A, representative competition curves for the CB receptor agonist WIN55,212-2, the selective CB $_1$ receptor antagonist AM251, and CBD against 1 nM [^3H]SR141716A (a selective CB $_1$ receptor antagonist) binding to cortical membranes. Points are means \pm S.E.M. of triplicate points. B, agonist-binding curves for the CB receptor agonist WIN55,212-2, the selective CB $_1$ receptor antagonist AM251, and CBD stimulation of [^{35}S]GTP γ S binding to cortical membranes. Points are means \pm S.E.M. of triplicate points from three separate experiments.

Finally, we investigated potential functional effects of CBD using [³⁵S]GTPγS binding assays in rat cortical membranes; CBD actions were compared with effects of WIN55,212-2 and AM251 (Fig. 7B). We first confirmed the presence of functional CB receptors. Accordingly, WIN55,212-2 caused an increase in percent stimulation of [³⁵S]GTPγS binding with an EC₅₀ of 95.1 ± 0.1 nM (*n* = 3); for 10 μM WIN55,212-2, *E*_{max} = 98.6 ± 3.5% (*n* = 3). AM251 had no stimulatory effect on [³⁵S]GTPγS binding at tested concentrations of <1 μM; at micromolar concentrations AM251 caused a moderate depression of [³⁵S]GTPγS binding (10 μM AM251: -20.3 ± 4.3%, *n* = 3). CBD had no effect at concentrations ≤1 μM; large decreases in [³⁵S]GTPγS binding were seen at 10 μM CBD (-28.8 ± 10.3%, *n* = 3) and 100 μM CBD (-76.7 ± 15.9%, *n* = 3).

Thus, overall, CBD had clear antiepileptogenic and antiseizure effects but only low affinity and no clear agonist effects at cortical CB₁ receptors.

Discussion

CBD Reduces Excitability in in Vitro Models of Epileptiform Activity. In the present study, we use extracellular MEA recordings to demonstrate that CBD attenuates epileptiform activity in both the Mg²⁺-free and 4-AP in vitro models of status epilepticus in the mammalian hippocampus, a prominent epileptogenic region (Ben-Ari and Cossart, 2000). The major effects of CBD were to decrease LFP burst amplitude and duration in a hippocampal region-specific manner. In general, the CA1 region was most sensitive to CBD effects. Thus, LFP amplitude was significantly reduced at lower CBD concentrations in CA1 than in CA3 (with DG remaining unaffected) in Mg²⁺-free aCSF, and CA1 was the only region in which LFP amplitude was affected in 4-AP aCSF. This is of interest because the CA1 region represents the major output of the hippocampus, relaying information to cortical and subcortical sites and is intimately involved in propagation of epileptic activity (McCormick and Contreras, 2001). Contour plots constructed from data in the Mg²⁺-free and 4-AP models confirmed that LFP bursts typically originated in the CA3 region and propagated toward CA1 (Feng and Durand, 2005), strongly suggesting that CA1 is a major focus of epileptic activity in the two models used and illustrating that CBD exerts a significant antiepileptiform effect in this region.

Overall, CBD induced more prominent effects in Mg²⁺-free than in 4-AP aCSF. This result may reflect inherent differences between the two models, which affect NMDA glutamate receptors and K⁺ channels, respectively. CBD had contrasting actions on LFP burst frequency between models; frequency was increased in all regions by CBD in Mg²⁺-free aCSF but was decreased in all regions in 4-AP aCSF. It is interesting to note that 100 μM CBD was without effect on burst frequency in the Mg²⁺-free model, in contrast to data for all the lower concentrations of CBD tested. This finding was the only indication of any biphasic action of CBD, a common phenomenon associated with cannabinoids whereby increasing concentrations cause changes in the pharmacological “direction” of action (Pertwee, 2008).

In light of the region-specific effects of CBD, it will be of interest in the future to investigate the cellular mechanisms of action of CBD using intracellular recording from individual neurons in selected hippocampal regions. In both the Mg²⁺-free and 4-AP models, contour plots and subsequent analyses showed that CBD caused clear attenuation in LFP burst amplitude but had no overall effect on burst propagation speed. These findings suggest that CBD acts to reduce the magnitude of epileptiform activity while leaving speed of information transmission across the hippocampal slice intact. It is possible that this action may result in a more tolerable side effect profile for CBD in comparison with existing AEDs if used in a clinical setting.

CBD Has Anticonvulsant Properties in the PTZ Model of Generalized Seizures.

CBD had beneficial effects on seizure severity and lethality in response to PTZ administration without delaying the time taken for seizures to develop. CBD (100 mg/kg) demonstrated clear anticonvulsant effects in terms of significant reductions in median seizure severity, tonic-clonic seizures, and mortality. Particularly striking effects were that <10% of animals developed tonic-clonic seizures or died when treated with CBD in comparison to approximately 50% of vehicle-treated animals. The present data strongly substantiate a number of earlier *in vivo* studies suggesting that CBD has anticonvulsant potential ([Lutz, 2004](#); [Scuderi et al., 2009](#)). CBD has been reported to have relatively potent anticonvulsant action in maximal electroshock (a model of partial seizure with secondary generalization) ([Karler et al., 1974](#); [Consroe and Wolkin, 1977](#)). Moreover, CBD prevented tonic-clonic seizures in response to electroshock current ([Consroe et al., 1982](#)). There are limited clinical data on CBD effects on seizure frequency in humans ([Gordon and Devinsky, 2001](#)). However, in one small double-blind study of eight patients with uncontrolled secondary generalized epilepsy treated with 200 to 300 mg of CBD, four remained symptom-free and three had signs of improvement ([Cunha et al., 1980](#)). One potential concern was the high doses of CBD used by [Cunha et al. \(1980\)](#). Because all new therapies must be introduced initially in an adjunct capacity to existing medication, the present study suggests that one attractive possibility is a role for CBD as an adjunct in generalized seizures. In this regard, earlier animal studies indicate that CBD enhances the effects of phenytoin (although CBD reduced the potency of other AEDs) ([Consroe and Wolkin, 1977](#)). In the future, it will be of interest to extend studies to other animal seizure models and also to combination therapies with selective AEDs to determine the full clinical anticonvulsant potential of CBD against a range of epilepsy phenotypes.

Mechanism of Action. Cannabinoid actions are mediated by CB₁ and CB₂ receptors, potentially by the GPR55 receptor, and also by cannabinoid receptor-independent mechanisms ([Howlett et al., 2004](#); [Ryberg et al., 2007](#)). In regard to epilepsy, CB₁ receptors are densely expressed in the hippocampal formation ([Herkenham et al., 1990](#); [Tsou et al., 1998](#)) where their activation is widely reported to be antiepileptic in animal models ([Shen and Thayer, 1999](#); [Wallace et al., 2001](#); but see [Clement et al., 2003](#)). Here, we demonstrate that CBD displaced the selective CB₁ receptor antagonist [³H]SR141716A in cortical membranes with relatively low affinity ($K_i = 1.82 \mu\text{M}$); these data are in line with values reported in whole brain membranes (reviewed in [Pertwee, 2008](#)) and our data in cerebellar membranes ([Smith et al., 2009](#)). CB receptor/G-protein coupling may differ among distinct brain regions ([Breivogel et al., 1997](#); [Dennis et al., 2008](#)); therefore, we investigated CBD effects on [³⁵S]GTP γ S binding in isolated cortical membranes. We showed that CBD has no stimulatory agonist activity but that CBD at micromolar concentrations decreases G protein activity. These findings are also in agreement with studies in mouse whole brain membranes ([Thomas et al., 2007](#)), which showed that CBD has only low affinity at CB₁ and CB₂ receptors but acts efficaciously as an antagonist at both receptor types ([Thomas et al., 2007](#); see [Pertwee, 2008](#)). There are a number of potential mechanisms by which ligands acting at CB receptors may mediate anticonvulsant effects. Receptor agonists may act at CB₁ on excitatory presynaptic terminals to inhibit glutamate neurotransmitter release. Such a mechanism is unlikely here as CBD has no agonist effect in GTP γ S binding assays ([Thomas et al., 2007](#)). An alternative is that antagonists act at CB₁ receptors on inhibitory presynaptic terminals to increase GABA release. We have demonstrated such a mechanism for the phytocannabinoid Δ^9 -tetrahydrocannabivarin in the cerebellum ([Ma et al., 2008](#)), where displacement of eCB tone may lead to increased inhibition. It may also be speculated that the decreases in G protein activity seen in GTP γ S binding assays represent an inverse agonist action at CB₁ receptors; for example, if CBD were acting as an inverse agonist at CB₁ receptors on inhibitory presynaptic terminals an increase in GABA release could lead to reduced excitability. However, mechanisms involving increases in GABA release are unlikely here as CBD was effective in reducing seizures *in vivo* in the presence of the GABA_A receptor antagonist PTZ. Moreover, CBD-induced reductions in [³⁵S]GTP γ S binding to whole brain membranes were retained in CB₁ knockout [*cnr1*(-/-)] mice, suggesting that CBD is not an inverse agonist at CB₁

receptors (Thomas et al., 2007). Overall, the low affinity and lack of agonist activity at CB₁ receptors suggests that the CBD anticonvulsant effects reported here are potentially mediated by CB₁ receptor-independent mechanisms. In addition to the study of Thomas et al., showing that CBD actions were unaltered in *cnr1*(^{-/-}) mice, CBD anticonvulsant effects in the maximal electroshock model were unaffected by the CB₁ receptor antagonist SR141716A, whereas those of Δ⁹-THC and WIN55,212-2 were blocked (Wallace et al., 2001).

In addition to CB receptors, a number of alternative molecular targets may also contribute to CBD effects on neuronal excitability. CBD has been reported to be an antagonist at GPR55, a non-CB₁/CB₂ receptor (Ryberg et al., 2007); in contrast, a recent study demonstrated that CBD has no effect at GPR55 (Kapur et al., 2009). CBD may cause an increase in anticonvulsant eCBs via the reported inhibition of the catabolic enzyme fatty acid hydrolyase, which degrades anandamide, and/or the blockade of anandamide uptake (Watanabe et al., 1996; Rakhshan et al., 2000; Bisogno et al., 2001). CBD is reported to be a weak agonist at human TRPV1 receptors (Bisogno et al., 2001); a more recent study suggests an action for CBD at rat and human transient receptor potential vanilloid 2 but not rat transient receptor potential vanilloid 1 receptors (Qin et al., 2008). More relevant to potential effects on neuronal excitability in the CNS is the demonstration that CBD exerts a bidirectional action on [Ca²⁺]_i levels in hippocampal neurons (Ryan et al., 2009). Under control conditions, CBD induces increases in [Ca²⁺]_i; in contrast, in the presence of 4-AP (which induces seizure-like [Ca²⁺]_i oscillations) or increased extracellular K⁺, CBD acts to reduce [Ca²⁺]_i and thus epileptiform activity, via an action on mitochondria Ca²⁺ stores. A further recent report provides the first evidence that CBD can also block low-voltage-activated (T-type) Ca²⁺ channels (Ross et al., 2008), important modulators of neuronal excitability. Finally, CBD may also enhance the activity of inhibitory glycine receptors (Ahrens et al., 2009). Overall, the demonstration that CBD acts on multiple molecular targets that each play a key role in neuronal excitability reinforces the potential of CBD as an AED.

In conclusion, our data in separate in vitro models of epileptiform activity and, in particular, the beneficial reductions in seizure severity caused by CBD in an in vivo animal model of generalized seizures suggests that earlier, small-scale clinical trials for CBD in untreated epilepsy warrant urgent renewed investigation.

Supplementary Material

Data Supplement:

[Click here to view.](#)

Acknowledgments

We thank Professor Philip Strange for useful discussion and Colin Stott (GW Pharmaceuticals) and Professor Gernot Riedel (University of Aberdeen) for pharmacokinetics data.

This work was supported by a GW Pharmaceuticals and Otsuka Pharmaceuticals award, by a University of Reading Research Endowment Trust Fund award; and The Wellcome Trust [Grant 070739].

Article, publication date, and citation information can be found at <http://jpet.aspetjournals.org>.

doi:10.1124/jpet.109.159145

□ The online version of this article (available at <http://jpet.aspetjournals.org>) contains supplemental material.

ABBREVIATIONS:

CNS central nervous system

CB cannabinoid

eCB endocannabinoid

Δ^9 -THC Δ^9 -tetrahydrocannabinol

CBD cannabidiol

AED antiepileptic drug

MEA multielectrode array

aCSF artificial cerebrospinal fluid

4-AP 4-aminopyridine

LFP local field potential

NMDA *N*-methyl-D-aspartate

BSA bovine serum albumin

SR141716A *N*-(piperidin-1-yl)-5-(4-chlorophenyl)-1-(2,4-dichlorophenyl)-4-methyl-1*H*-pyrazole-3-carboxamide

AM251 *N*-(piperidin-1-yl)-5-(4-iodophenyl)-1-(2,4-dichlorophenyl)-4-methyl-1*H*-pyrazole-3-carboxamide

GTP γ S guanosine 5'-O-(3-thio)triphosphate

WIN55,212-2 [2,3-dihydro-5-methyl-3-(4-morpholinylmethyl)pyrrolo[1,2,3-*de*]-1,4-benzoxazin-6-yl]-1-naphthalenylr

PTZ pentylenetetrazole.

References

- Abramoff MD, Magelhaes PJ, Ram SJ. (2004) Image processing with ImageJ. *J Biophoton Int* 11:36–42 [[Google Scholar](#)]
- Ahrens J, Demir R, Leuwer M, de la Roche J, Krampfl K, Foadi N, Karst M, Haeseler G. (2009) The nonpsychotropic cannabinoid cannabidiol modulates and directly activates $\alpha 1$ and $\alpha 1\beta$ glycine receptor function. *Pharmacology* 83:217–222 [[PubMed](#)] [[Google Scholar](#)]
- Ben-Ari Y, Cossart R. (2000) Kainate, a double agent that generates seizures: two decades of progress. *Trends Neurosci* 23:580–587 [[PubMed](#)] [[Google Scholar](#)]
- Bhattacharyya S, Fusar-Poli P, Borgwardt S, Martin-Santos R, Nosarti C, O'Carroll C, Allen P, Seal ML, Fletcher PC, Crippa JA, et al. (2009) Modulation of mediotemporal and ventrostriatal function in humans by Δ^9 -tetrahydrocannabinol: a neural basis for the effects of *Cannabis sativa* on learning and psychosis. *Arch Gen Psychiatry* 66:442–451 [[PubMed](#)] [[Google Scholar](#)]
- Bisogno T, Hanus L, De Petrocellis L, Tchilibon S, Ponde DE, Brandi I, Moriello AS, Davis JB, Mechoulam R, Di Marzo V. (2001) Molecular targets for cannabidiol and its synthetic analogues: effect on vanilloid VR1 receptors and on the cellular uptake and enzymatic hydrolysis of anandamide. *Br J Pharmacol* 134:845–852 [[PMC free article](#)] [[PubMed](#)] [[Google Scholar](#)]
- Blair RE, Deshpande LS, Sombati S, Falenski KW, Martin BR, DeLorenzo RJ. (2006) Activation of the cannabinoid type-1 receptor mediates the anticonvulsant properties of cannabinoids in the hippocampal neuronal culture models of acquired epilepsy and status epilepticus. *J Pharmacol Exp Ther* 317:1072–1078 [[PubMed](#)] [[Google Scholar](#)]
- Breivogel CS, Sim LJ, Childers SR. (1997) Regional differences in cannabinoid receptor/G-protein coupling in rat brain. *J Pharmacol Exp Ther* 282:1632–1642 [[PubMed](#)] [[Google Scholar](#)]
- Clement AB, Hawkins EG, Lichtman AH, Cravatt BF. (2003) Increased seizure susceptibility and proconvulsant activity of anandamide in mice lacking fatty acid amide hydrolase. *J Neurosci* 23:3916–3923 [[PubMed](#)] [[Google Scholar](#)]
- Consroe P, Benedito MA, Leite JR, Carlini EA, Mechoulam R. (1982) Effects of cannabidiol on behavioral seizures caused by convulsant drugs or current in mice. *Eur J Pharmacol* 83:293–298 [[PubMed](#)] [[Google Scholar](#)]

- Consroe P, Wolkin A. (1977) Cannabidiol-antiepileptic drug comparisons and interactions in experimentally induced seizures in rats. *J Pharmacol Exp Ther* 201:26–32 [[PubMed](#)] [[Google Scholar](#)]
- Cunha JM, Carlini EA, Pereira AE, Ramos OL, Pimentel C, Gagliardi R, Sanvito WL, Lander N, Mechoulam R. (1980) Chronic administration of cannabidiol to healthy volunteers and epileptic patients. *Pharmacology* 21:175–185 [[PubMed](#)] [[Google Scholar](#)]
- Dennis I, Whalley BJ, Stephens GJ. (2008) Effects of Δ^9 -tetrahydrocannabivarin on [^{35}S]GTP γ S binding in mouse brain cerebellum and piriform cortex membranes. *Br J Pharmacol* 154:1349–1358 [[PMC free article](#)] [[PubMed](#)] [[Google Scholar](#)]
- Egert U, Heck D, Aertsen A. (2002a) Two-dimensional monitoring of spiking networks in acute brain slices. *Exp Brain Res* 142:268–274 [[PubMed](#)] [[Google Scholar](#)]
- Egert U, Knott T, Schwarz C, Nawrot M, Brandt A, Rotter S, Diesmann M. (2002b) MEA-Tools: an open source toolbox for the analysis of multi-electrode data with MATLAB. *J Neurosci Methods* 117:33–42 [[PubMed](#)] [[Google Scholar](#)]
- Farrimond JA, Hill AJ, Jones NA, Stephens GJ, Whalley BJ, Williams CM. (2009) A cost-effective high-throughput digital system for observation and acquisition of animal behavioral data. *Behav Res Methods* 41:446–451 [[PubMed](#)] [[Google Scholar](#)]
- Feng Z, Durand DM. (2005) Decrease in synaptic transmission can reverse the propagation direction of epileptiform activity in hippocampus *in vivo*. *J Neurophysiol* 93:1158–1164 [[PubMed](#)] [[Google Scholar](#)]
- Gordon E, Devinsky O. (2001) Alcohol and marijuana: effects on epilepsy and use by patients with epilepsy. *Epilepsia* 42:1266–1272 [[PubMed](#)] [[Google Scholar](#)]
- Hampson AJ, Grimaldi M, Axelrod J, Wink D. (1998) Cannabidiol and (-) Δ^9 -tetrahydrocannabinol are neuroprotective antioxidants. *Proc Natl Acad Sci U S A* 95:8268–8273 [[PMC free article](#)] [[PubMed](#)] [[Google Scholar](#)]
- Herkenham M, Lynn AB, Little MD, Johnson MR, Melvin LS, de Costa BR, Rice KC. (1990) Cannabinoid receptor localization in brain. *Proc Natl Acad Sci U S A* 87:1932–1936 [[PMC free article](#)] [[PubMed](#)] [[Google Scholar](#)]
- Hill AJ, Jones NA, Williams CM, Stephens GJ, Whalley BJ. (2009) Development of multi-electrode array screening for anticonvulsants in acute rat brain slices. *J Neurosci Methods* doi:10.1016/j.jneumeth.2009.10.007 [[PubMed](#)] [[Google Scholar](#)]
- Howlett AC, Breivogel CS, Childers SR, Deadwyler SA, Hampson RE, Porrino LJ. (2004) Cannabinoid physiology and pharmacology: 30 years of progress. *Neuropharmacology* 47:345–358 [[PubMed](#)] [[Google Scholar](#)]
- Iuvone T, Esposito G, De Filippis D, Scuderi C, Steardo L. (2009) Cannabidiol: a promising drug for neurodegenerative disorders? *CNS Neurosci Ther* 15:65–75 [[PMC free article](#)] [[PubMed](#)] [[Google Scholar](#)]
- Kapur A, Zhao P, Sharir H, Bai Y, Caron MG, Barak LS, Abood ME. (2009) Atypical responsiveness of the orphan receptor GPR55 to cannabinoid ligands. *J Biol Chem* 284:29817–29827 [[PMC free article](#)] [[PubMed](#)] [[Google Scholar](#)]
- Karler R, Cely W, Turkkanis SA. (1974) Anticonvulsant properties of Δ^9 -tetrahydrocannabinol and other cannabinoids. *Life Sci* 15:931–947 [[PubMed](#)] [[Google Scholar](#)]
- Kwan P, Brodie MJ. (2007) Emerging drugs for epilepsy. *Expert Opin Emerg Drugs* 12:407–422 [[PubMed](#)] [[Google Scholar](#)]
- Löscher W, Hönack D, Fassbender CP, Nolting B. (1991) The role of technical, biological and pharmacological factors in the laboratory evaluation of anticonvulsant drugs. III. Pentylentetrazole seizure models. *Epilepsy Res* 8:171–189 [[PubMed](#)] [[Google Scholar](#)]
- Lowry OH, Rosebrough NJ, Farr AL, Randall RJ. (1951) Protein measurement with the Folin phenol reagent. *J Biol Chem* 193:265–275 [[PubMed](#)] [[Google Scholar](#)]

- Ludányi A, Eross L, Czirják S, Vajda J, Halász P, Watanabe M, Palkovits M, Maglóczy Z, Freund TF, Katona I. (2008) Downregulation of the CB₁ cannabinoid receptor and related molecular elements of the endocannabinoid system in epileptic human hippocampus. *J Neurosci* 28:2976–2990 [[PubMed](#)] [[Google Scholar](#)]
- Lutz B. (2004) On-demand activation of the endocannabinoid system in the control of neuronal excitability and epileptiform seizures. *Biochem Pharmacol* 68:1691–1698 [[PubMed](#)] [[Google Scholar](#)]
- Ma YL, Weston SE, Whalley BJ, Stephens GJ. (2008) The phytocannabinoid Δ^9 -tetrahydrocannabinol modulates inhibitory neurotransmission in the cerebellum. *Br J Pharmacol* 154:204–215 [[PMC free article](#)] [[PubMed](#)] [[Google Scholar](#)]
- McCormick DA, Contreras D. (2001) On the cellular and network bases of epileptic seizures. *Annu Rev Physiol* 63:815–846 [[PubMed](#)] [[Google Scholar](#)]
- Mechoulam R, Shvo Y. (1963) Hashish. I. The structure of cannabidiol. *Tetrahedron* 19:2073–2078 [[PubMed](#)] [[Google Scholar](#)]
- Monory K, Massa F, Egertová M, Eder M, Blaudzun H, Westenbroek R, Kelsch W, Jacob W, Marsch R, Ekker M, et al. (2006) The endocannabinoid system controls key epileptogenic circuits in the hippocampus. *Neuron* 51:455–466 [[PMC free article](#)] [[PubMed](#)] [[Google Scholar](#)]
- Pertwee RG. (2008) The diverse CB₁ and CB₂ receptor pharmacology of three plant cannabinoids: Δ^9 -tetrahydrocannabinol, cannabidiol and Δ^9 -tetrahydrocannabinol. *Br J Pharmacol* 153:199–215 [[PMC free article](#)] [[PubMed](#)] [[Google Scholar](#)]
- Pohl M, Mares P. (1987) Effects of flunarizine on metrazol-induced seizures in developing rats. *Epilepsy Res* 1:302–305 [[PubMed](#)] [[Google Scholar](#)]
- Qin N, Neepser MP, Liu Y, Hutchinson TL, Lubin ML, Flores CM. (2008) TRPV2 is activated by cannabidiol and mediates CGRP release in cultured rat dorsal root ganglion neurons. *J Neurosci* 28:6231–6238 [[PubMed](#)] [[Google Scholar](#)]
- Rakhshan F, Day TA, Blakely RD, Barker EL. (2000) Carrier-mediated uptake of the endogenous cannabinoid anandamide in RBL-2H3 cells. *J Pharmacol Exp Ther* 292:960–967 [[PubMed](#)] [[Google Scholar](#)]
- Ross HR, Napier I, Connor M. (2008) Inhibition of recombinant human T-type calcium channels by Δ^9 -tetrahydrocannabinol and cannabidiol. *J Biol Chem* 283:16124–16134 [[PMC free article](#)] [[PubMed](#)] [[Google Scholar](#)]
- Ryan D, Drysdale AJ, Lafourcade C, Pertwee RG, Platt B. (2009) Cannabidiol targets mitochondria to regulate intracellular Ca²⁺ levels. *J Neurosci* 29:2053–2063 [[PubMed](#)] [[Google Scholar](#)]
- Ryberg E, Larsson N, Sjögren S, Hjorth S, Hermansson NO, Leonova J, Elebring T, Nilsson K, Drmota T, Greasley PJ. (2007) The orphan receptor GPR55 is a novel cannabinoid receptor. *Br J Pharmacol* 152:1092–1101 [[PMC free article](#)] [[PubMed](#)] [[Google Scholar](#)]
- Sagredo O, Ramos JA, Decio A, Mechoulam R, Fernández-Ruiz J. (2007) Cannabidiol reduced the striatal atrophy caused 3-nitropropionic acid *in vivo* by mechanisms independent of the activation of cannabinoid, vanilloid TRPV1 and adenosine A2A receptors. *Eur J Neurosci* 26:843–851 [[PubMed](#)] [[Google Scholar](#)]
- Scuderi C, Filippis DD, Iuvone T, Blasio A, Steardo A, Esposito G. (2009) Cannabidiol in medicine: a review of its therapeutic potential in CNS disorders. *Phytother Res* 23:597–602 [[PubMed](#)] [[Google Scholar](#)]
- Shen M, Thayer SA. (1999) Δ^9 -Tetrahydrocannabinol acts as a partial agonist to modulate glutamatergic synaptic transmission between rat hippocampal neurons in culture. *Mol Pharmacol* 55:8–13 [[PubMed](#)] [[Google Scholar](#)]
- Smith I, Bevan SA, Whalley BJ, Stephens GJ. (2009) Phytocannabinoid affinities at CB₁ receptors in the mouse cerebellum. *Proceedings of the 19th Annual Meeting of the International Cannabinoid Research Society; 2009 July 8–11; Pheasant Run, St. Charles, IL. P81, International Cannabinoid*

Research Society; [[Google Scholar](#)]

- Stett A, Egert U, Guenther E, Hofmann F, Meyer T, Nisch W, Haemmerle H. (2003) Biological application of microelectrode arrays in drug discovery and basic research. *Anal Bioanal Chem* 377:486–495 [[PubMed](#)] [[Google Scholar](#)]
- Straiker A, Mackie K. (2005) Depolarization-induced suppression of excitation in murine autaptic hippocampal neurones. *J Physiol* 569:501–517 [[PMC free article](#)] [[PubMed](#)] [[Google Scholar](#)]
- Thomas A, Baillie G, Philips AM, Razdan RK, Ross RA, Pertwee RG. (2007) Cannabidiol displays unexpectedly high potency as an antagonist of CB₁ and CB₂ receptor agonists *in vitro*. *Br J Pharmacol* 150:917–926 [[PMC free article](#)] [[PubMed](#)] [[Google Scholar](#)]
- Tsou K, Brown S, Sañudo-Peña MC, Mackie K, Walker JM. (1998) Immunohistochemical distribution of cannabinoid CB₁ receptors in the rat central nervous system. *Neuroscience* 83:393–411 [[PubMed](#)] [[Google Scholar](#)]
- Vivo M, Lin H, Strange PG. (2006) Investigation of cooperativity in the binding of ligands to the D₂ dopamine receptor. *Mol Pharmacol* 69:226–235 [[PubMed](#)] [[Google Scholar](#)]
- Wallace MJ, Martin BR, DeLorenzo RJ. (2002) Evidence for a physiological role of endocannabinoids in the modulation of seizure threshold and severity. *Eur J Pharmacol* 452:295–301 [[PubMed](#)] [[Google Scholar](#)]
- Wallace MJ, Wiley JL, Martin BR, DeLorenzo RJ. (2001) Assessment of the role of CB₁ receptors in cannabinoid anticonvulsant effects. *Eur J Pharmacol* 428:51–57 [[PubMed](#)] [[Google Scholar](#)]
- Watanabe K, Kayano Y, Matsunaga T, Yamamoto I, Yoshimura H. (1996) Inhibition of anandamide amidase activity in mouse brain microsomes by cannabinoids. *Biol Pharm Bull* 19:1109–1111 [[PubMed](#)] [[Google Scholar](#)]
- Whalley BJ, Stephens GJ, Constanti A. (2009) Investigation of the effects of the novel anticonvulsant compound carisbamate (RWJ-333369) on rat piriform cortical neurones *in vitro*. *Br J Pharmacol* 156:994–1008 [[PMC free article](#)] [[PubMed](#)] [[Google Scholar](#)]

Articles from The Journal of Pharmacology and Experimental Therapeutics are provided here courtesy of
American Society for Pharmacology and Experimental Therapeutics